Astrochemistry: From Molecular Clouds to Planetary Systems
IAU Symposium, Vol. 197, 2000
Y. C. Minh and E. F. van Dishoeck, eds.

ISO's View of the Molecular Content of Evolved Stars

J. Cernicharo
CSIC. IEM. Dpt. Molecular Physics, C/Serrano 121, 28006 Madrid, Spain

Abstract. The recent results of the ISO satellite in the field of molecular spectrocopy of AGB stars are reviewed. For the fist time, the two spectrometers onboard ISO have provided the opportunity to observe the pure rotational lines of several molecules in the far infrared and the ro-vibrational bands of the most abundant molecular species in the near and mid-infrared. These data allow to carry out a systematic study of the circumstellar envelopes of AGB stars and Planetary Nebulae. I analyze in this paper the role of resonant scatterring in the pumping of the ro-vibrational molecular levels in CSEs.

1. Introduction

While polar molecules can be detected at radio wavelengths, non-polar molecules can only be detected in the infrared through their active ro-vibrational transitions. On the other hand, observations of the vibrational bands of polar molecules complement the radio data providing essential constraints to the modelling of the observations, and to the determination of the physical and chemical conditions of the molecular gas in the circumstellar envelopes (CSE) of AGB stars. Some physical processes, like radiative pumping of molecular levels, which are very important in the energetic balance of the CSEs can be traced only at infrared wavelengths.

The ISO-SWS spectrometer (de Graauw et al. 1996) covers the 2.38–45 μm wavelength range, allowing a systematic search for the presence of nearly all likely abundant molecular species through their stretching and/or bending vibrational bands. The ISO-LWS spectrometer (Clegg et al. 1996) covers the 44–197 μm wavelength range and permits to observe the pure rotational lines of species like CO, H_2O, HCN,... The spectral resolution provided by the SWS full resolution grating observations, R=1500–2000, permits to resolve the rotational structure of the molecular bands arising from molecules with rotational constants larger than 0.2 cm^{-1} – i.e. from practically all diatomic and triatomic species and from some four-atomic molecular species. The SWS and LWS complement the already available ro-vibrational data obtained from ground based telescopes and allow the study of vibrational bands and pure rotational lines for which the observation from ground-based telescopes is difficult, or even impossible, due to the low atmospheric transmission at these wavelengths.

2. The Warm Layers of the Circumstellar Envelopes of AGB Stars

In comparison with the millimeter/submillimeter domains where up to now most of the studies have been made, the near-, mid- and far-IR range provide a unique opportunity to probe the inner hottest regions of the CSE. The observation of molecular transitions involving high quantum numbers at far-IR wavelengths and the observation of hot- and combination-bands in the near and mid-infrared allow to trace the molecular material in the innermost zones of the CSE. Tsuji et al. (1997) have analyzed the ISO-SWS spectra in the direction of M giants and Miras. They found that the stretching band of water vapour at 2.7 μm and the CO_2 stretching band at 4.2 μm appear in absorption in these objects. The analysis of these molecular bands indicates excitation temperatures around 750−1250 K. Tsuji et al. (1997) suggest that these features are produced in a rather warm molecule-forming region above the photosphere that could be related to the quasi-static molecular zone previously observed from high resolution observations of CO, C_2H_2 and other molecular species (Keady & Hinkle 1988; Keady & Ridway 1993). This warm molecular zone is very close to the star and has also been observed in the near and mid-IR ISO's spectrum of IRC+10216 (Cernicharo et al. 1999a; see below). Yamamura et al. (1999a) have observed SO_2 in some O-rich objects. They have modelled the observations with very simple assumptions that allow to reproduce the shape of the band as a function of the stellar phase. They conclude that SO_2 is very abundant in the innermost regions of O-rich CSEs and that the different ISO data indicate the presence of several warm layers of high density which could be related to the dynamical processes associated with stellar pulsation. However, their models are too simple because they neglect some important physical processes, like radiative pumping effects, on the population of the ro-vibrational levels of these molecular species (González-Alfonso & Cernicharo 1999a,b). We will discuss these effects in the sections devoted to HCN in IRC+10216 and to H_2O in O-rich stars.

3. Carbon-rich AGB Stars: The Case of IRC+10216

IRC+10216 is the brightest C-rich evolved object in the sky and is the prototype of C-rich AGB objects. It has an extended CSE where around 50 molecular species have been detected, and it is probably one of the best studied stellar objects at infrared and radio wavelengths (Cernicharo, Guélin, & Kahane 2000). IRC+10216 has a particularly rich carbon chemistry, in such a way that most of the species detected in this source are carbon chain radicals (C_5H: Cernicharo et al. 1986a,b, 1987a; C_6H: Suzuki et al. 1986, Guélin et al. 1987, Cernicharo et al. 1987b; C_8H: Cernicharo & Guélin 1996; C_7H: Guélin et al. 1997; H_2C_3 and H_2C_4: Cernicharo et al 1991a,b; C_5N: Guélin, Neininger, & Cernicharo 1998) which are formed in the external layers of the CSE (Guélin, Lucas, & Cernicharo 1993). Other species of interest detected in IRC+10216 include silicon carbide (SiC; Cernicharo et al. 1989a), the metal-bearing molecules, such as the metal halides NaCl, AlCl, AlF, and KCl, detected for the first time in this CSE by Cernicharo & Guélin (1987), NaCN (Turner, Steimle, & Meerts 1994). Some metal-bearing species were also detected in the external shell of IRC+10216: MgNC (Ishii et al. 1993; Guélin et al. 1986; Guélin, Lucas, & Cernicharo 1993) and MgCN (Ziurys

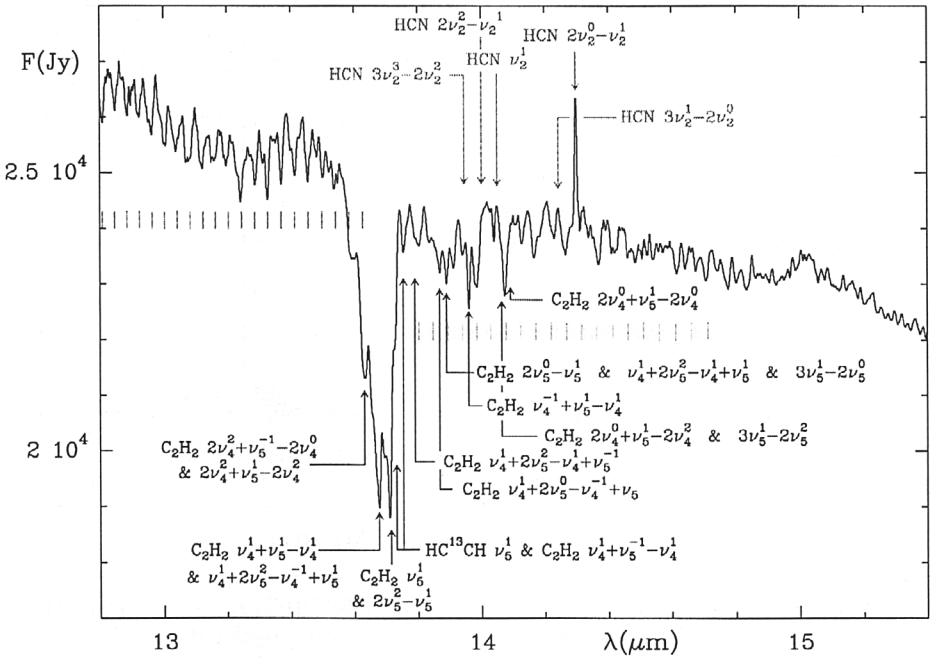

Figure 1. Observed ISO-SWS spectrum of IRC+10216 around 15 μm. Spectral resolution is $\simeq 200$ km s^{-1}. The positions of the bands are indicated. Vertical lines indicated the position of the individual R and P lines of the fundamental bending mode of C_2H_2. Note that the HCN bands are in emission as indicated by the shape of the P–band of C_2H_2 relative to the R one and by the strong Q–band of the $2\nu_2$ l=0 – ν_2 l=1 transition.

et al. 1995). The emission from the innermost regions of the CSE of IRC+10216 seems to indicate a chemistry in thermodynamical equilibrium (Tsuji 1973). Most of the stable diatomic, triatomic and also many polyatomic species are formed efficiently in these layers (CO, HCN, C_2H_2, SiO, CS, SiS, ...).

3.1. The near and mid-infrared spectrum of IRC+10216

Cernicharo et al. (1999a) have observed IRC+10216 with the ISO-SWS spectrometer. They have found a broad absorption feature at 3 μm which is due to the stretching modes of C_2H_2 and HCN. In addition, the Q–branches of the $\nu_3+\nu_5$, $\nu_3+\nu_4$ and $\nu_2+2\nu_4+\nu_5$ modes of C_2H_2 are detected around 2.5 μm. Many combination bands of the same molecule, like $\nu_2+\nu_5$ among others, are detected around 3.8 μm. The Q–branch of the $\nu_2+\nu_3$ mode of HCN and those of the $\nu_1+\nu_2$ and $\nu_1+2\nu_2-\nu_2$ vibrational transitions of HCN are detected in absorption around 2.5 μm and 3.6 μm respectively. The $\nu_3-\nu_2$ mode of HCN and other combination bands are also detected (see their Figure 2). By assuming an LTE distribution of the C_2H_2 and HCN level populations, they modelled the absorption produced by 21 bands of C_2H_2 and 2 bands of $H^{13}CCH$, together with three bands of HCN and the ν_3 band of $H^{13}CN$. Cernicharo et al. (1999a) conclude

https://doi.org/10.1017/S0074180900164952 Published online by Cambridge University Press

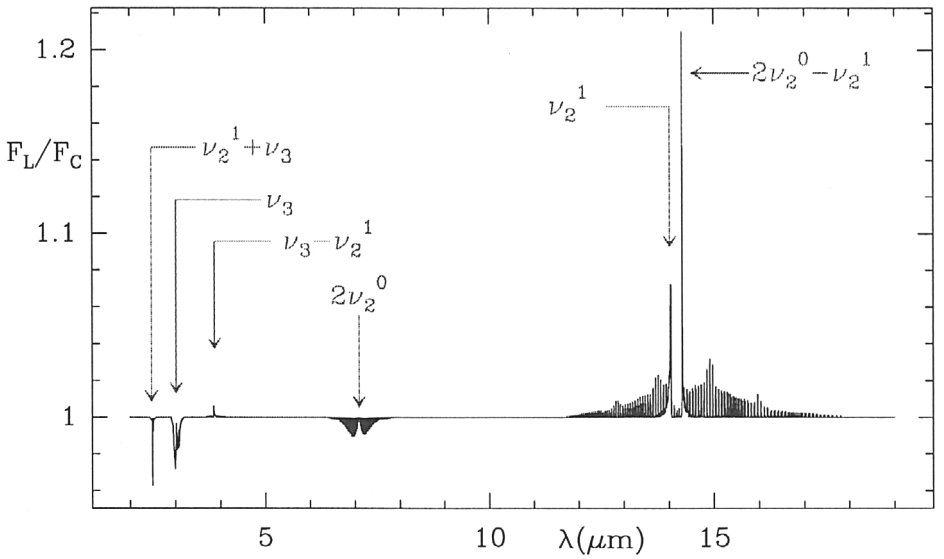

Figure 2. Modelled HCN spectrum in IRC+10216. The model is described in the text. Note the large intensity predicted for the Q–band of the $2\nu_2$ l=0 – ν_2 l=1 transition in good agreement with the observations. In addition, the (0,0,1)–(0,1^1,0) band is also predicted in emission (from Cernicharo et al. 1999a and González-Alfonso & Cernicharo 1999a).

that a model with a single layer cannot explain the observed band profile (see Keady & Hinkle 1988). They adopted the detailed CSE structure derived by Keady & Hinkle and X(C_2H_2)=5 10^{-5} and X(HCN)=3 10^{-5} (from Cernicharo et al. 1996, Wiedemann et al. 1991; see below). In order to fit the wings of the 3 μm feature they needed to include an additional contribution from warm gas in the inner region ($T_K \approx 1700$ K; $1 < r < 3$ R_*). This layer could be similar to the warm molecular envelope found by Tsuji et al. (1997) in other CSEs (see also above) and its origin is probably related to the pulsation of the central star (Woitke et al. 1999).

Figure 1 shows the 14 μm spectrum of IRC+10216 (Cernicharo et al. 1999a). The absorption features are due to the ν_5 bending mode of acetylene and its associated hot and combination bands. This figure shows that the HCN bands appear in emission with the Q-branch of the $2\nu_2^0-\nu_2^1$ transition being particularly strong. The HCN emission has to be modelled in a more complicated way than C_2H_2. The ν_3 band of HCN at 3 μm is seen in absorption (Cernicharo et al. 1999a) whereas the bending states are detected in emission against the continuum. P-Cygni profiles are in fact expected for HCN and C_2H_2 (Wiedemann et al. 1991). The larger beam size of the SWS compared to the high angular resolution data of Wiedemann et al. could favour the observation of re-emission from HCN through resonant scattering in the molecular envelope.

The different behaviour of the bending bands of C_2H_2 and HCN must be related to the larger abundance of C_2H_2 through the whole envelope (which in-

https://doi.org/10.1017/S0074180900164952 Published online by Cambridge University Press

creases the importance of stellar blocking, and absorption by the dust due to the larger number of absorption and re-emision processes; see González-Alfonso & Cernicharo 1999a,b) and/or to the excitation mechanism that gives rise to the HCN band emission. Cernicharo et al. conclude that an important difference between both molecules would be established if rovibrational excitation is mainly radiative, instead of collisional: while the $2\nu_2^0$ state of HCN is radiatively connected to the ground state, the equivalent transition in C_2H_2 is forbidden, i.e., no photons can be absorbed from the ground to the $2\nu_5^0$ state due to the fact that both levels have the same symmetry. In HCN, photons absorbed from the ground to the $2\nu_2^0$ level will decay preferently to the ν_2^1 level, because the Einstein coefficient for spontaneous emission of this transition is ~ 4 s^{-1}, i.e., twice the value corresponding to the decay to the ground state. The equivalent process in C_2H_2 is radiative excitation from the ground to the $\nu_4+\nu_5$ state followed by radiative decay to the ν_4 level. However, this transition is very close in frequency to the Q-branch of the ν_5 transition, and any possible reemission could not compensate the strong absorption from the ground to the ν_5 bending mode.

By using the non-local, non-LTE code developed by González-Alfonso & Cernicharo (1997), Cernicharo et al. (1999a) have modelled the HCN emission/absorption in IRC+10216. The results (see Figure 2) predict that the ν_3, $\nu_3+\nu_2$ and the $2\nu_2$ bands of HCN will be in absorption while the ν_2 and its overtone bands will be in emission. The model also predicts that the $\nu_3-\nu_2$ band will be in emission as observed by Cernicharo et al. The best fit to the data was obtained with an HCN abundance of $\sim(1$–$1.5)\ 10^{-5}$ which is only a factor of two smaller than that derived from the ISO-LWS data (see below). The pumping mechanisms are different for the different regions of the envelope. In the innermost regions, before the dust formation zone, absorption of photons at 3 μm in the ν_3 mode will be very efficient. Radiative decay to the $2\nu_2$ l=0 and ν_2 l=1 states will be an important mechanism to populate both levels. Also in this region the $\nu_3-\nu_2$ band will appear in emission. Outside the dust formation region the flux at 3 μm decreases but it increases considerably at 7.1 μm. The pumping from the ground state to the $2\nu_2$ l=0 vibrational level, followed by radiative decay to the ν_2 l=1 level, will be the main mechanism in producing the observed emission at 14.3 μm. Consequently, the intensity of the HCN bands, as observed by ISO, could be very different in stars with low, moderate or high mass loss rates (see, e.g. Aoki et al. 1999). These calculations show that resonant scattering through the envelope is very efficient for HCN and that it could also have an effect on the heating and cooling of the molecular gas (Cernicharo 1998).

3.2. The far-infrared spectrum of IRC+10216

Cernicharo et al. (1996) have observed the 43–197 μm spectrum of IRC+10216 as observed with the ISO-LWS. Figure 3 shows the continuum-subtracted LWS spectrum of IRC+10216 together with the results of a LVG model for CO and HCN (Cernicharo et al. 1996). The spectrum is dominated by the emission of carbon monoxide and HCN in all their vibrational states. Some lines of ^{13}CO and H^{13}CN are also detected. The CO lines are strong throughout the wavelength range of the LWS and only show a decrease in the intensity for the highest J

https://doi.org/10.1017/S0074180900164952 Published online by Cambridge University Press

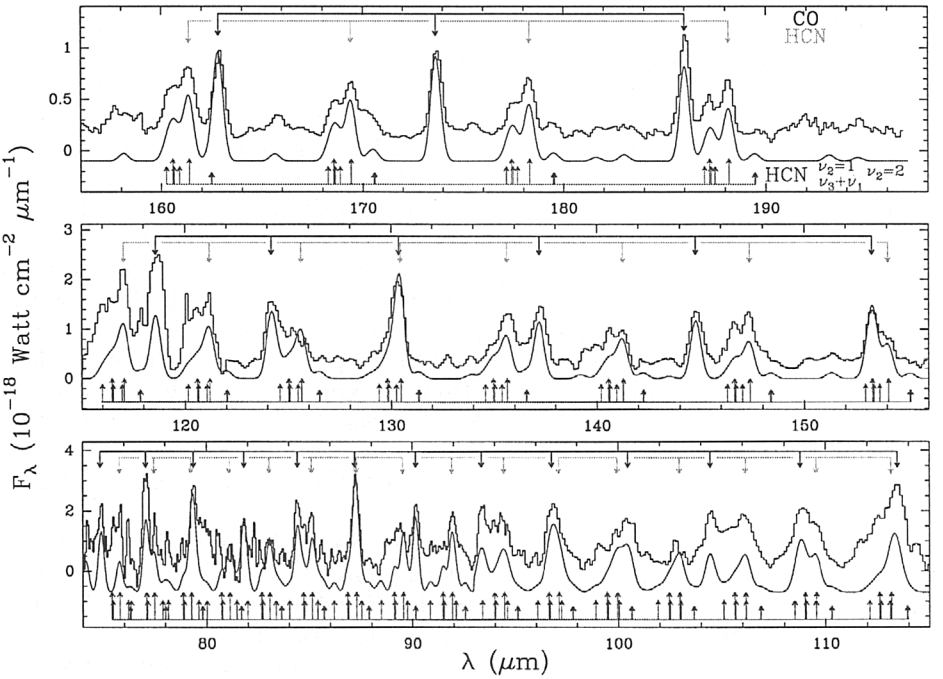

Figure 3. Continuum subtracted LWS grating spectrum of IRC+10216 from 75 to 197 μm (thick line). An offset has been introduced to the continuum to show simultaneously the computed emission of the CO v=0, 1, ^{13}CO v=0, HCN and H^{13}CN v=0, and HCN ν_2=1,2 $\nu_{1,3}$ =1 (thin line). The rotational transitions of CO, HCN, and HCN ν_2=1,2 and $\nu_{1,3}$=1 are indicated at the top and bottom of each panel. The weak lines in the model correspond to H^{13}CN, ^{13}CO and to the stretching modes of HCN (from: Cernicharo et al. 1996).

rotational transitions. Besides the rotational lines of CO, a forest of HCN lines from different vibrational states were detected from J=18→17 to 48→47. HCN has a bending mode, ν_2, at $\simeq$713 cm^{-1}, and two stretching modes ν_1 and ν_3, at 2096 and 3311 cm^{-1} respectively. Cernicharo et al. (1996) concluded that after removing the CO lines, all the remaining strong features in the far-IR spectrum of IRC+10216 are due to HCN. Some of the weak features remaining in the far-IR spectrum of IRC+10216 could be assigned to rotational transitions of CS and SiO. However, the limited spectral resolution of the data in Figure 3 avoids any certain identification for these features. Cernicharo et al. (1996) searched for NaH, MgH, CaH, NH, CH, FeH, NiH, SH, SiH, CH_2, and other light molecular species without success. However, they reported a tentative detection of the Q(2,4,6,8) lines of the bending mode of triatomic carbon, C_3, around 157.2 μm (Cernicharo et al., in preparation). Some weak and broad features present in Figure 3 could also correspond to the ν_2=1,2 levels of H^{13}CN.

The most spectacular result from the ISO-LWS spectrum of IRC+10216 is the forest of lines arising from the different vibrational levels of HCN. This result could have been expected on the basis of the strong maser emission found by

https://doi.org/10.1017/S0074180900164952 Published online by Cambridge University Press

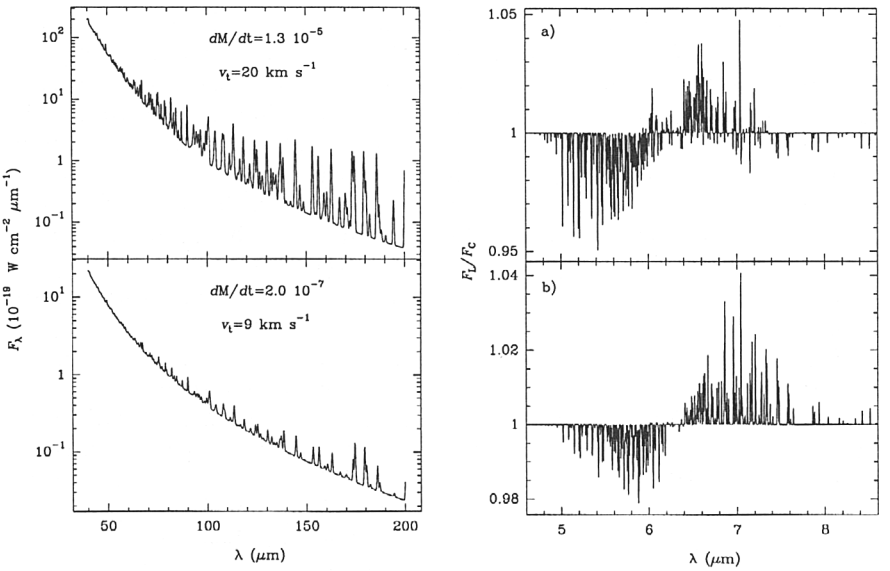

Figure 4. *(left panels)* Expected LWS spectrum in O-rich stars for high (upper panel) and low mass loss rates (lower panel). The models include the the pure rotational lines of H_2O and CO. *(right panels)* Expected SWS spectrum around 6 μm for the two models shown in the left panels (González-Alfonso & Cernicharo 1999b). The predicted behaviour of the bending mode of water vapour has been observed in the direction of high mass star-forming regions (González-Alfonso et al. 1998).

Lucas & Cernicharo (1989) in the ν_2=1 state and the strong thermal emission in the J=2→1 and J=3→2 lines from the other vibrational levels of HCN. The best agreement between the observations and the model results (which are shown in Figure 3) is obtained for HCN/CO=0.1 which corresponds to an HCN abundance of 3 10^{-5}, a value that agrees with that derived from millimeter observations (Cernicharo et al. 1987a). Taking into account the uncertainties associated with the data calibration and with the baseline used to remove the continuum, the agreement between the observations and our model results is reasonably good. In the far-IR, $\lambda > 70$ μm, the power emitted in the HCN lines is 0.44 $L_\odot$ while that of CO is 0.28 $L_\odot$ (even when the millimeter and sub-millimeter lines of CO and HCN are included). Hence HCN is the main coolant in the inner regions of this C-rich CSE. HCN plays in C-rich AGB stars a similar role to that of water in O-rich CSEs. Ryde et al. (1999a) have also observed the CO far-IR lines with ISO in the C-rich object IRAS15194-5115.

4. Oxygen-rich AGB Stars

About 30 pure rotational lines of water vapour have been detected in the oxygen-rich AGB star W Hya by Barlow et al. (1996). A similar study of R Cas has been carried out by Truong-Bach et al. (1999). Unlike the spectrum of IRC+10216,

https://doi.org/10.1017/S0074180900164952 Published online by Cambridge University Press

the far-infrared spectrum of O-rich stars is dominated by the emission of the rotational lines of H_2O. Taking into account the large variation of the temperature and density profiles across the envelopes, these lines, which cover a very large range of energies and Einstein coefficients, could provide the best tool to derive the physical conditions of the gas in these objects. The water vapour abundance derived from the modelling of the data in W Hya is 10^{-4}. Neufeld et al. (1996) have observed 4 high excitation transitions of H_2O with the SWS-FP spectrometer in the same object but reached different values for the mass loss rate of the star due to the different temperature profile adopted in their modelling, which shows the strong dependence of the intensity of the H_2O pure rotational lines with the physical conditions in the CSE of O-rich objects.

The ro-vibrational transitions of the bending mode of H_2O, together with the stretching mode of OH between 3–3.5 μm and the stretching mode of CO_2 at 4.2 μm, were observed for the first time in the evolved star NML Cyg by Justtanont et al. (1996) using the SWS spectrometer. Far-IR OH lines have been observed in IRC+10420 by Sylvester et al. (1997). They analyse the role of these lines in the pumping of the OH maser transitions.

ISO-SWS data of large sample of O-rich stars have been analyzed by Matsuura et al. (1999). Yamamura et al. (1999b) have observed the stretching mode of water vapour in Mira and in Z Cas. In the former object they found the band in emission while in the latter it is observed in absorption. Using an LTE approximation they conclude that the different behaviour of the vibrational band is due to the different size of the H_2O warm layer around the central star. The densities needed to fill the LTE assumption, like in the case of CO_2 (Justtanont et al. 1998; Ryde et al. 1999b) and of SO_2 (Yamamura et al. 1999b), are very high but roughly consistent with dynamical model atmospheres (Woitke et al. 1999). These LTE plane-parallel models are in fact very simple and, due to the lack of spectral resolution, depend on only three parameters: the excitation temperature, the size of the molecular layer and the molecular abundance. However, they neglect all pumping mechanisms other than collisions (which they assume large enough to quasi-thermalize the vibrational levels). Due to the selection rules associated with vibrational transitions prevailing for the bending and overtone modes of triatomic molecules, these models cannot account for some of the observed properties of the H_2O, CO_2 and HCN (see above) and in particular for the important role of radiative pumping through the absorption of photons from the central object and its surrounding dust. González-Alfonso & Cernicharo (1999a,b) have modelled the H_2O emission in O-rich stars with the use of non-LTE and non-Local codes that allow to treat simultaneously dust and molecules. Figure 4a shows the computed far-IR spectrum (pure rotational lines) for two different mass loss rates and terminal velocities. In both cases the distance to the star is 500 pc and the water vapour abundance is assumed to be 2.5 10^{-4}. The radius of the star and of the envelope are 3.5 10^{13} and 10^{17} cm respectively. The stellar temperature is 2500 K. The spectrum shown in the bottom panel could apply to W Hya (see Barlow et al. 1996) when the fluxes are corrected for the distance of this object (100 pc). The top panel of Figure 4a applies for a star with very large mass loss rate like VX Sgr or VY CMa (after a distance correction). The CO lines are much weaker than those of H_2O for the mass loss rate of W Hya but become comparable to the H_2O lines for dM/dt as

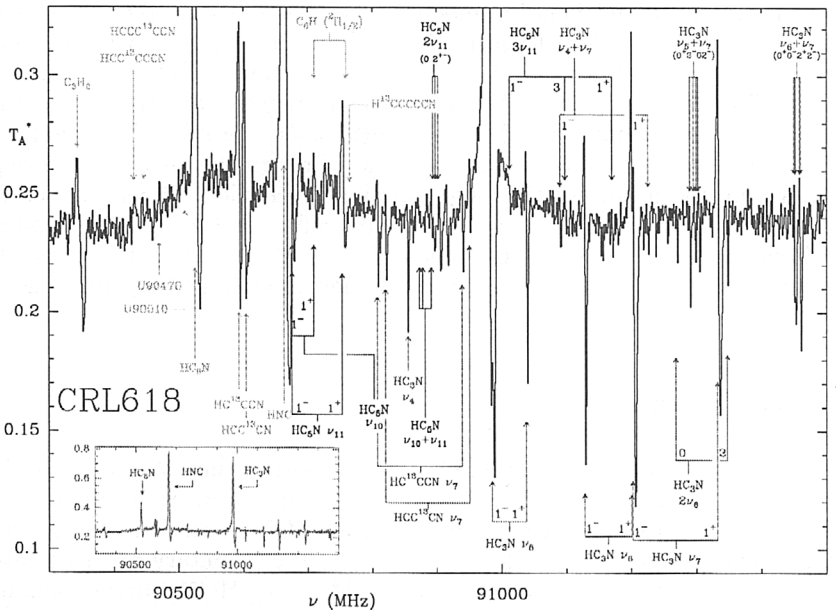

Figure 5. The spectrum of CRL618 around 91000 MHz as observed with the 30-m IRAM radio telescope. Most of the absorption lines are due to ro-vibrational lines of HC_3N and HC_5N.

high as 10^{-5} $M_\odot$ yr^{-1}. The cooling of the gas is dominated in these objects by the emission of pure rotational lines of water vapour.

Figure 4b shows the results for the bending mode of H_2O at 6 μm. Some ro-vibrational lines will be seen in absorption while many others will be in emission. Resonant scattering through the envelope is responsible for this behaviour. For stars with very high mass-loss rates the band will be seen in absorption. However, for medium and low mass loss rates the band will have a profile similar to the plots in Figure 4b (see González-Alfonso & Cernicharo 1999a,b for details). Resonant scattering will have a very important role in the heating of the gas in the region where collisions between the vibrational levels are negligible but where collisions inside the ground state can repopulate its rotational levels. A photon absorbed in the ground level will pump the molecule to a given level in the bending vibrational level. Reemission to one of the allowed rotational levels in the ground state, followed by collisional de-excitation in the ground state, will put energy in the gas phase. The region where this mechanism applies corresponds to that of densities larger than a few 10^5 cm^{-3}, but low enough to have negligible vibrational excitation through collisions. In stars with low mass loss rate this region is located near the photosphere while in stars with very high mass loss rate it starts at 10–20 stellar radii.

In the near infrared Justtanont et al. (1996) have reported the detection of CO_2 in gas phase at 4.3 μm in NML Cyg. In the same object they have also identified the bending and stretching modes of H_2O. Several pure rotational lines were also observed in emission. Recently, Justannont et al. (1998) have discovered strong CO_2 emission around 15 μm corresponding to vibrational transitions

https://doi.org/10.1017/S0074180900164952 Published online by Cambridge University Press

between stretching and bending modes. The CO_2 emission seems to be correlated with the 13 μm dust feature. They argue that there is a warm gas layer (650−1250 K) where both the 13 μm feature dust and the CO_2 emission lines are formed. The existence of such a warm layer has also been claimed by Tsuji et al. (1997) in their study with the SWS spectrometer of several M giants. However, detailed analysis of resonant scattering through the envelope are required to determine the nature of the CO_2 emission. González-Alfonso & Cernicharo (1999a) have computed the expected band-profile for the bending modes and associated hot- and combination-bands of CO_2 at 15 μm and concluded that resonant scattering cannot be neglected when modelling the pumping of the ro-vibrational bands of CO_2.

5. Post-AGB Stars

Cox et al. (1996) and Liu et al. (1996) have reported the LWS spectra of CRL 2688 and NGC7027. The CRL2688 far-infrared spectrum is dominated by the emission of CO with a weak contribution from HCN lines. It is due to the fact that the central star has started its evolution to the planetary nebula phase and that the innermost part of the envelope, where strong HCN emission is found in IRC+10216, has been removed. In NGC7027 the emission is completely dominated by CO and atomic fine structure lines. The high velocity wind associated with the evolution to the planetary phase and the UV photons from the central bright star perturb the circumstellar envelope in these objects producing shocks and photodissociation regions (PDRs) which modify the physical and chemical conditions of the gas (Cernicharo et al. 1989a; Neri et al. 1992; Herpin & Cernicharo 1999).

CRL618 is a C-rich star evolving very fast towards the planetary nebula stage. The molecular content of the circumstellar envelope of this object, as observed at millimeter wavelengths, is very similar to that of IRC+10216, i.e., long carbon radicals like C_4H and C_6H, cyanopolyynes such as HC_3N, HC_5N, HC_7N, and HC_9N, etc. However, its millimeter spectrum presents a remarkable difference with respect to IRC+10216: pure rotational lines of highly excited vibrational states of HC_3N and HC_5N produce a forest of absorption lines that are not present in IRC+10216 (Cernicharo et al. 1999b and Figure 5). Only the low energy ν_7 mode of HC_3N and perhaps the lowest energy ν_{11} mode of HC_5N are detected in IRC+10216. CRL618 also presents an extremely high velocity wind, covering 400 km s^{-1} (Cernicharo et al. 1989b), that perturbs the CSE from its AGB phase producing shocked regions, where molecules can be destroyed and reformed under very different physical conditions than those prevailing in the AGB phase (see Cernicharo et al. 1989a,b; Neri et al. 1992). As a consequence of this activity, CRL618 is the only C-rich object where H_2CO has been detected (see Cernicharo et al. 1989a,b).

Although the difference in the spectrum between both objects can be explained as due to different physical conditions, the millimeter data indicate the presence of molecules that are not detected in IRC+10216: CH_3C_2H and CH_3C_4H. Moreover, the column densities for the long cyanopolyynes are higher than in IRC+10216. The infrared spectrum of both sources could reveal the richness of their molecular content and of their physical and chemical conditions.

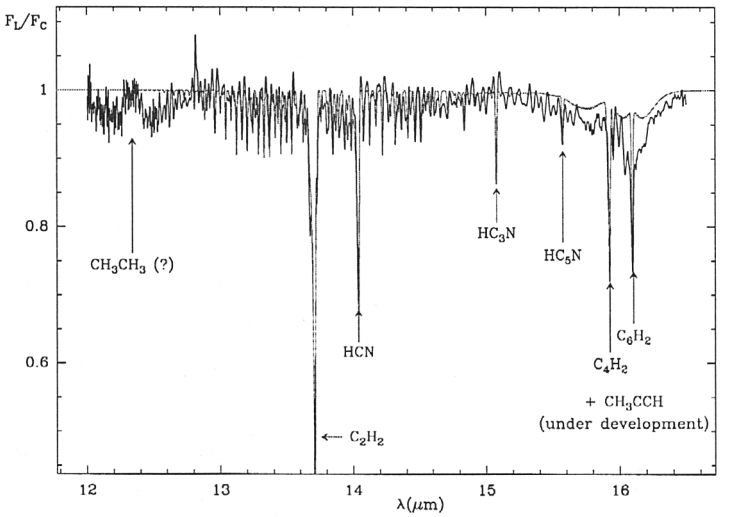

Figure 6. The SWS spectrum of CRL618 around 15 μm. The narrow features around 16 μm are due to C_4H_2 and C_6H_2.

Figure 6 shows the spectrum of CRL618 around 15 μm which has to be compared with that of IRC+10216 shown in Figure 1. The spectra are completely different. Only the fundamental bending modes of C_2H_2 and HCN are detected. In addition, the spectrum presents several narrow features corresponding to the Q-branches of the bending modes of HC_3N, HC_5N and, for the first time in interstellar space, to the bending modes of C_4H_2 and C_6H_2. These two molecular species have strong combination bands around 8 μm that are very prominent in the SWS spectrometer data —see Cernicharo et al. (1999b). The lowest energy bending modes of HC_3N and C_4H_2 are also detected at 45 μm with the LWS spectrometer.

The column densities of these species are around (5–10) 10^{16} cm^{-2}, i.e., only a factor of 10–20 below that of C_2H_2. The corresponding abundance ratio in IRC+10216 between C_2H_2 and C_4H_2 is larger than 100, which shows that important physical processes have modified the chemistry of CRL618. Moreover, and in agreement with the millimeter wave observations, the HC_3N and HC_5N Q-branches are not detected in IRC+10216, which indicates the very large abundances of these species in CRL618. C_4H_2 and C_6H_2 have also been detected in CRL2688, another proto-planetary nebula.

In addition to these species, NH_3 produces an impressive forest of absorption bands around 10 μm. These bands are blended with those from C_2H_4. CH_4, C_3H_2 and a combination band of C_2H_2 also contributes to the absorption bands around 8 μm (Cernicharo et al. 1999b). The ISO-SWS spectrum of CRL618 is dominated by a very large number of absorption bands that remain unidentified. Many of them could arise from small hydrocarbons like $(CH_3)_2$, $(CH_3)_2CH_2$, CH_3, CH_2, CH_3CCH, etc. We are working on the identification of these features, but an important input from laboratory data is needed.

https://doi.org/10.1017/S0074180900164952 Published online by Cambridge University Press

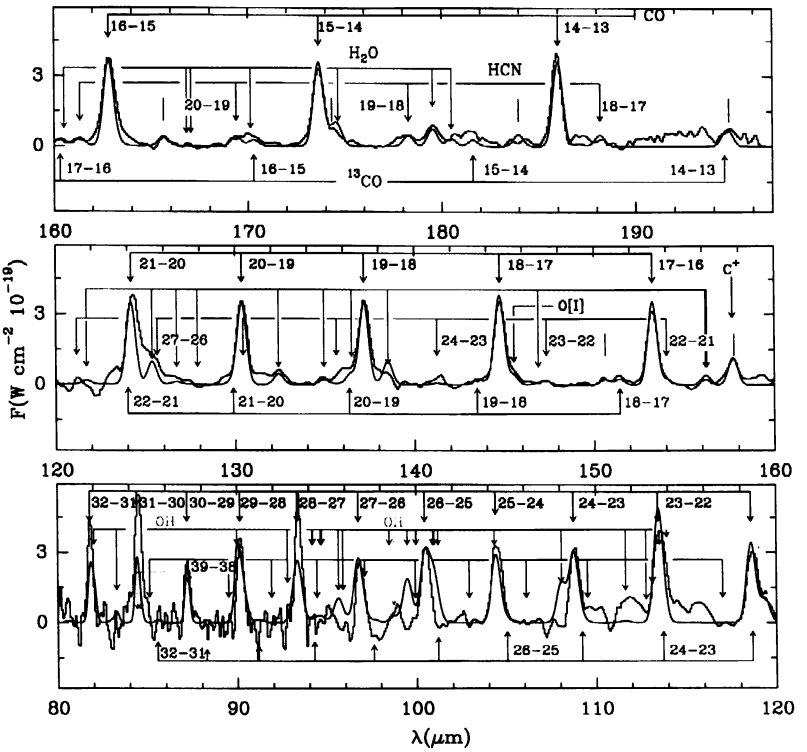

Figure 7. Continuum subtracted ISO-LWS spectra of CRL618. The result of a multispatial component model is shown by the continuous line. The lines of CO, ^{13}CO, HCN, H_2O and OH are indicated by arrows while those of HNC are indicated by vertical lines (from J=22–21 at 150.627 μm to J=17–16 at 194.759 μm) (from: Herpin & Cernicharo 1999).

Herpin & Cernicharo (1999) have analysed the LWS spectrum of CRL618. In addition to the lines of CO, ^{13}CO, HCN and HNC, they report the detection of H_2O and OH emission together with the fine structure lines of [OI] at 63 and 145 μm (see Figure 7). The derived abundances for these O-bearing species, relative to CO, are 4 10^{-2}, 8 10^{-4} and 4.5.

From an analysis of the structure of the envelope, and using an LVG model, they have obtained a reasonable fit to the data (see Figure 7). They suggest that O-bearing species other than CO are produced in the innermost region of the circumstellar envelope. The UV photons from the central star, together with the high velocity winds prevailing in CRL618, destroy most of the molecular species produced in the AGB phase and allow a chemistry dominated by standard ion-neutral reactions. Not only do these reactions allow the formation of O-bearing species but they also modify the abundances of C-rich molecules like HCN and HNC for which we found an abundance ratio of $\simeq 1$, much lower than in AGB stars. Hence, CRL618 shows an enormous variety of carbon chains and small hydrocarbons together with O-bearing species like H_2O, OH, HCO^+ and H_2CO.

https://doi.org/10.1017/S0074180900164952 Published online by Cambridge University Press

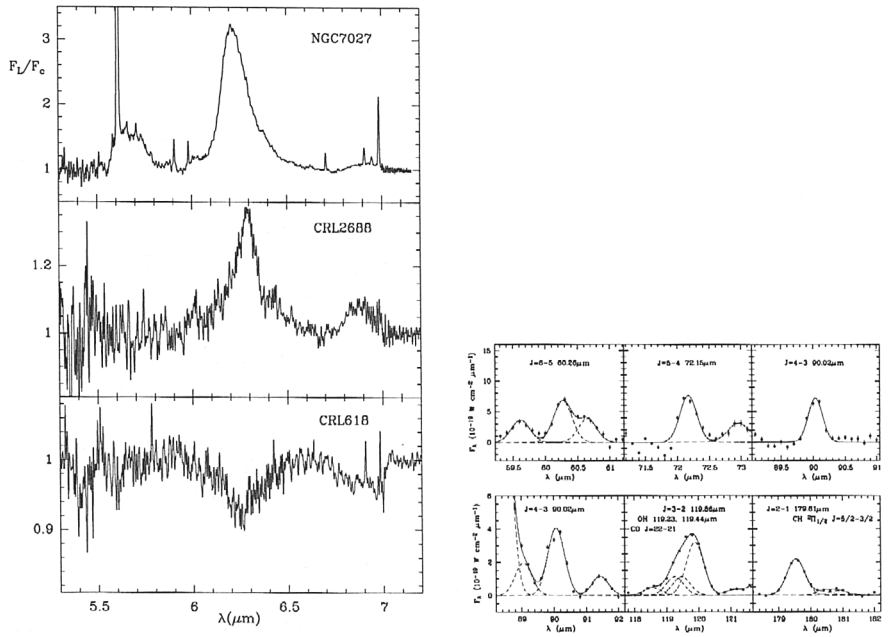

Figure 8. *(right panels)* The SWS spectrum of NGC7027, CRL2688 and CRL618 around 6 μm. A baseline, resulting from a fit to the continuum emission, has been removed from the three spectra. *(left panels)* CH^+ lines observed in NGC7027. The solid lines are Gaussian line profile fits to the observed features (for blends, contributions from individual components are shown as dashed lines). The J=2→1 line at 179.62 μm was previously assigned to H_2O (from: Cernicharo et al. 1997).

Finally, the comparison of the spectrum of NGC7027, CRL2688 and CRL618 at 6 μm (see Figure 8a) indicates that the region where the UIBs appear in emission is, in the case of CRL618, dominated by several absorption bands with clear vibrational structure. Although we have not found yet potential carriers for the broad absorption around 6 μm, we believe that it is produced by several carbon-rich gas phase molecules of moderate size. The detection of long carbon chains and small hydrocarbons in CRL618 and CRL2688 suggests that in the proto-planetary stage of C-rich stars, the extremely high velocity winds associated with the evolution of these objects, and the strong UV field from the central star, could modify the chemistry of the CSE. A large variety of small molecules are formed during this stage. They could be the pieces from which large carbon-rich macromolecules could form and produce the UIBs through excitation by UV photons. Alternatively, all these species, including the carriers of the UIBs, could be released to the gas phase from the dust grains under the action of the strong shocks, and of the UV photons, to which the innermost envelope is submitted.

https://doi.org/10.1017/S0074180900164952 Published online by Cambridge University Press

5.1. CH^+ in Planetary Nebulae

CH^+ was one of the first molecules detected in astrophysics through its $^1\Pi$–$^1\Sigma$ electronic transition at optical wavelengths. This molecule is abundant in the diffuse interstellar medium and during many years the chemical reactions involved in its formation have been subject of important controversy. Cernicharo et al. (1997) have reported the discovery of several pure rotational transitions of CH^+ in the LWS spectrum of NGC7027 (see Figure 8b). The strong line at 179.62 μm (nearly coincident in frequency with the 2_{12}–1_{01} transition of water vapour) and the lines at 119.90 and 90.03 μm (reported as unidentified by Liu et al. 1996), whose frequencies are in harmonic relation 2 : 3 : 4, arise from the J=2→1, 3→2, and 4→3 rotational transitions of CH^+. This identification is strengthened by the detection in the LWS spectra of the next two rotational lines of CH^+, at 72.17 and 60.22 μm. Cernicharo et al. (1997) have derived a rotational temperature for the CH^+ lines of 160 K, a volume density of a few 10^7 cm^{-3}, and a CH^+/CO abundance ratio of (0.2–1) 10^{-3}. Given the carbon-rich nature of NGC7027 and the strong UV radiation field in its inner regions it is thus not too surprising to find CH^+ in this prototypical PN. However, this is the first time that CH^+ has been seen through its pure rotational spectrum. Taking into account the dipole moment of CH^+ (1.7 D) and the energy of its rotational levels, the rotational transitions of this molecular species constitute a unique tool to trace the physical conditions of the PDRs of the interstellar and circumstellar medium.

6. Conclusions

ISO has opened a new view of the near-, mid- and far-IR spectra of evolved stars providing useful constraints to the modelling of the CSEs of these objects. An important conclusion from the modelling of these data is the crucial role of radiative pumping in populating the vibrational levels of molecular species. However, three important caveats still have to be addressed: (i) the absolute lack of collisional cross sections for the vibrational levels of most molecular species; (ii) the lack of laboratory data for the spectroscopy of most molecules of astrophysical interest, and (iii) ISO's poor spectral resolution which cannot separate the different spatial contributions to the emission/absorption features produced by the molecules. The latter one will be solved when the FIRST satellite will fly in 2007. The HIFI heterodyne instrument that will be installed onboard FIRST will have a very high spectral resolution ($\Delta\lambda/\lambda$ better than 10^{-6}), excellent frequency coverage (0.5–3 THz) and very high sensitivity allowing the observation of less abundant species and the derivation of accurate line profiles for CO, HCN, H_2O and other molecular species. To solve the two first problems, however, we have to establish close collaborations with scientists doing quantum-mechanical calculations and laboratory spectroscopy work. Molecular Astrophysics is a multidisciplinary science and ISO is showing the importance of close collaboration among different physics and chemistry groups to derive the physical conditions of the gas in CSEs and in any warm environment of the interstellar medium.

Acknowledgments. I thank Spanish DGES and CICYT for support under grants PB96-0883 and ESP98-1351.

References

Aoki, W., Tsuji, T., & Ohnaka, K. 1999, A&A, 350, 945
Barlow, M.J., et al. 1996, A&A, 315, L241
Cernicharo, J. 1998, Astr. Space Science, 255, 303
Cernicharo, J., Barlow, M., González-Alfonso, E., et al. 1996, A&A, 315, 201
Cernicharo, J., Gottlieb, C.A., Guélin, M., et al. 1989a, ApJ, 341, L25
Cernicharo, J., Gottlieb, C.A., Guélin, M., et al. 1991a, ApJ, 368, L39
Cernicharo, J., Gottlieb, C.A., Guélin, M., et al. 1991b, ApJ, 368, L43
Cernicharo, J. & Guélin, M. 1987, A&A, 183, L10
———— 1996, A&A, 309, L27
Cernicharo, J., Guélin, M., & Kahane, C., 2000, A&A, in press
Cernicharo, J., Guélin, M., Menten, K., & Walmsley, C.M. 1987b, A&A, 181, L1
Cernicharo, J., Guélin, M., Peñalver, J., et al. 1989b, A&A, 222, L20
Cernicharo, J., Guélin, M., & Walmsley, C.M. 1987a, A&A, 172, L5
Cernicharo, J., Kahane, C., Gómez-González, J., & Guélin, M. 1986a, A&A, 164, L1
———— 1986b, A&A, 167, L5
Cernicharo, J., Liu, X.-W., González-Alfonso, E., et al. 1997, ApJ, 483, L65
Cernicharo, J., Yamamura, I., González-Alfonso, E., et al. 1999a, ApJ, 526, L21
Cernicharo J., et al. 1999b, in The Universe as seen by ISO, eds. P. Cox & M.F. Kessler (ESA SP-427, March 1999, Paris), 285
Clegg, P.E., et al. 1996, A&A, 315, L38
Cox, P., González-Alfonso, E., Barlow, M., et al. 1996, A&A, 315, L265
de Graauw Th., et al. 1996, A&A, 315, L49
González-Alfonso, E. & Cernicharo, J. 1997, A&A, 322, 938
———— 1999a, in The Universe as seen by ISO, eds. P. Cox & M.F. Kessler (ESA SP-427, March 1999, Paris), 325
———— 1999b, ApJ, 525, 845
González-Alfonso, E., Cernicharo, J., van Dishoeck, E.F., et al. 1998, ApJ, 502, L169
Guélin, M., Cernicharo, J., Kahane, C., & Gómez-González, J. 1986, A&A, 157, L17
Guélin, M., Cernicharo, J., Kahane, C., Gómez-González, J., & Walmsley, C.M. 1987, A&A, 175, L5
Guélin, M., Cernicharo, J. & Travers, M.J. 1997, A&A, 317, L1
Guélin, M., Lucas, R. & Cernicharo, J. 1993, A&A, 280, L19
Guélin, M., Neininger, N. & Cernicharo, J. 1998, A&A, 335, L1
Herpin, F. & Cernicharo, J. 1999, ApJ Letters, submitted.
Ishii, K., Hirano, T., Nagashima, U., Weis, B., & Yamashita, K. 1993, ApJ, 410, L43
Justtanont, K., de Jong, T., Helmich, F.P., et al. 1996, A&A, 315, L217
Justtanont, K., de Jong, T., Helmich, F.P., et al. 1998, A&A, 330, L17
Keady, J.J. & Hinkle, K.H. 1988, ApJ, 331, 539
Keady, J.J. & Ridway, S.T. 1993, ApJ, 406, 199
Lucas, R. & Cernicharo, J. 1989, A&A, 218, L20

Liu, X.-W., Barlow, M.J., Nguyen-Q-Rieu, et al. 1996, A&A, 315, L257
Matsuura, M., Yamamura, I., Murakami, H., et al. 1999, A&A, 348, 579
Neri, R., et al. 1992, A&A, 262, 544
Neufeld, D.A., Chen, W., Melnick, G.J., et al. 1996, A&A, 323, L237
Ryde, N., Schoier, F.L., & Olofsson, H. 1999a, A&A, 345, 841
Ryde, N., Eriksson, K., & Gustafsson, B. 1999b, A&A, 341, 579
Suzuki, H., Ohishi, M., Kaifu, N., Ishikawa, S.I., & Kasuga, T. 1986, PASJ, 38, 911
Sylvester, R.J., Barlow, M.J., Liu, X.-W., et al. 1997, MNRAS, 291, L42
Truong-Bach, Sylvester, R.J., Barlow, M.J., et al. 1999, A&A, 345, 925
Tsuji, T. 1973, A&A, 23, 411
Tsuji, T., Ohnaka, K., Aoki, W., & Yamamura, I. 1997, A&A, 320, L1
Turner, B., Steimle, T.C., & Meerts, L. 1994, ApJ, 426, L97
Wiedemann, G.R., Hinkle, K.H., Keady, J.J., et al. 1991, ApJ, 382, 321
Woitke, P., Helling, Ch., Winters, J.M., & Jeong, K.S. 1999, A&A, 348, L17
Yamamura, I., de Jong, T., & Cami, J. 1999a, A&A, 348, L55
Yamamura, I., de Jong, T., Onaka, T., Cami, J., et al. 1999b, A&A, 341, L9
Ziurys, L., Apponi, A.J., Cernicharo, J., & Guélin, M. 1995, ApJ, 445, L47

Discussion

A. Lapinov: (1) What fraction of C-stars has HCN J=2–1 masers? (2) What is the efficiency of IR pumping: what is the ratio of photons at the maser HCN J=2–1 transition to IR pumping photons? (3) Did you try to detect the maser effect in HNC?

J. Cernicharo: (1) We observed $\sim$40 objects. Masers are observed in 25 %. (2) I am not ready to answer this question now. (3) Not yet.

U. G. Jørgensen: Comment: very simplified models of the stellar atmosphere can often fit the spectra very well, but at the cost that we loose understanding of the star. The "3-layer-models" you refer to for analysing ISO spectra have at least 7 free parameters. They hide the very complicated structure of the photosphere that ISO spectra analysed with our fully self-consistent models reveal (e.g. Jørgensen, Hron, & Loidl 2000, A&A, in press, about the 14 μm band in carbon stars).